

Physical and electrical properties of Nb doped $\text{Bi}_{0.5}\text{Na}_{0.5}[\text{Zr}_{0.59}\text{Ti}_{0.41}]\text{O}_3$

Ampika Rachakom^a, Sukanda Jiansirisomboon^{a,b}, Anucha Watcharapasorn^{a,b,*}

^a Department of Physics and Materials Science, Faculty of Science, Chiang Mai University, 50200 Chiang Mai, Thailand

^b Materials Science Research Center, Faculty of Science, Chiang Mai University, 50200 Chiang Mai, Thailand

Available online 12 May 2011

Abstract

This research studied the effect of Nb doping on $\text{Bi}_{0.5}\text{Na}_{0.5}[\text{Ti}_{0.41}\text{Zr}_{0.59}]\text{O}_3$ (when Nb concentration = 0.00, 0.01, 0.03, 0.05, 0.07 and 0.09 mol fraction). Nb doped BNTZ ceramics were fabricated using a conventional mixed-oxide method. All samples were calcined at a temperature of 700 °C for 2 h and sintered at a temperature of 900 °C for 2 h. X-ray diffraction patterns suggested that the compounds possessed rhombohedral perovskite structure. SEM micrographs indicated that average grain size decreased as the amount of Nb additives increased. The electrical resistivity showed a decreasing trend with increasing Nb concentration due to excess charge present in the sample. The dielectric constant and dielectric loss of samples showed no particular trend when Nb was added but the optimum was observed when 0.05–0.07 Nb mol fraction was present in BNTZ ceramics. In this study, both microstructure and donor-type effects played an important role in determining electrical resistivity and dielectric properties of these ceramics.

© 2011 Elsevier Ltd and Techna Group S.r.l. All rights reserved.

Keywords: B. X-ray method; C. Dielectric properties; C. Electrical properties; Bismuth sodium titanate

1. Introduction

Currently, the most widely used piezoelectric materials are based on PbTiO_3 – PbZrO_3 ceramics. The most commonly used ceramic had a composition closed to morphotropic phase boundary (MPB) i.e. $\text{Zr}:\text{Ti} \sim 52:48$ [1–3], where properties such as piezoelectric coefficients and dielectric permittivity are maximized. Nevertheless, the main drawback of pure PZT material was its difficulties in being poled due to limited domain movement. In most cases, high-performance PZT ceramics are normally modified to enhance its dielectric, piezoelectric and ferroelectric properties using particular donor dopants such as Nb^{5+} to counteract the natural p-type conductivity of PZT [2], which was presumably caused by the lower-valence Fe ions inherently residing in the PZT lattice and unbalanced concentration of cationic and anionic defects [4]. This donor-ion substitution was then found to increase the electrical resistivity and improve poling efficiency [5–8]. However, the processing of PZT involves PbO which is considered not

environmentally friendly due to its toxicity. Therefore, several non-lead systems have recently been of interest in order to find a substitute for PZT. One such system is based on BaTiO_3 – BaZrO_3 [9,10] whose certain compositions were found to exhibit diffused phase transition and relaxor behavior. Another similar system involves $\text{Bi}_{0.5}\text{Na}_{0.5}\text{TiO}_3$ (BNT) and $\text{Bi}_{0.5}\text{Na}_{0.5}\text{ZrO}_3$ (BNZ). The former was known to show decent dielectric and piezoelectric properties [11,12]. The recent phase diagram of this BNT–BNZ system showed a possible MPB region near $\text{Zr}:\text{Ti} \sim 0.59:0.41$ [13]. Hence, in order to investigate the properties of this compound at MPB region as well as the effect of Nb doping, this research attempted to fabricate ceramics with a chemical formula $[\text{Bi}_{0.5}\text{Na}_{0.5}]_{1-x/2}[\text{Ti}_{0.41}\text{Zr}_{0.59}]_{1-x}\text{Nb}_x\text{O}_3$ where $x = 0.00, 0.01, 0.03, 0.05, 0.07$ and 0.09 mol fraction. The relationship between electrical properties, microstructures and crystal structure are reported and discussed.

2. Experimental procedures

The $[\text{Bi}_{0.5}\text{Na}_{0.5}]_{1-x/2}[\text{Ti}_{0.41}\text{Zr}_{0.59}]_{1-x}\text{Nb}_x\text{O}_3$ ceramics with $x = 0.00, 0.01, 0.03, 0.05, 0.07$ and 0.09 mol fraction were prepared by mixed-oxide method. The starting powders of Bi_2O_3 (>98%, Fluka), Na_2CO_3 (99.5%, Carlo Erba), TiO_2 (>99%, Riedel de Haën), ZrO_2 (>99%, Riedel de Haën) and Nb_2O_5 (99.9%, Aldrich) were mixed in ethanol using zirconia

* Corresponding author at: Department of Physics and Materials Science, Faculty of Science, Chiang Mai University, 50200 Chiang Mai, Thailand. Tel.: +66 53 941 921x632; fax: +66 53 892 271.

E-mail address: anucha@stanfordalumni.org (A. Watcharapasorn).

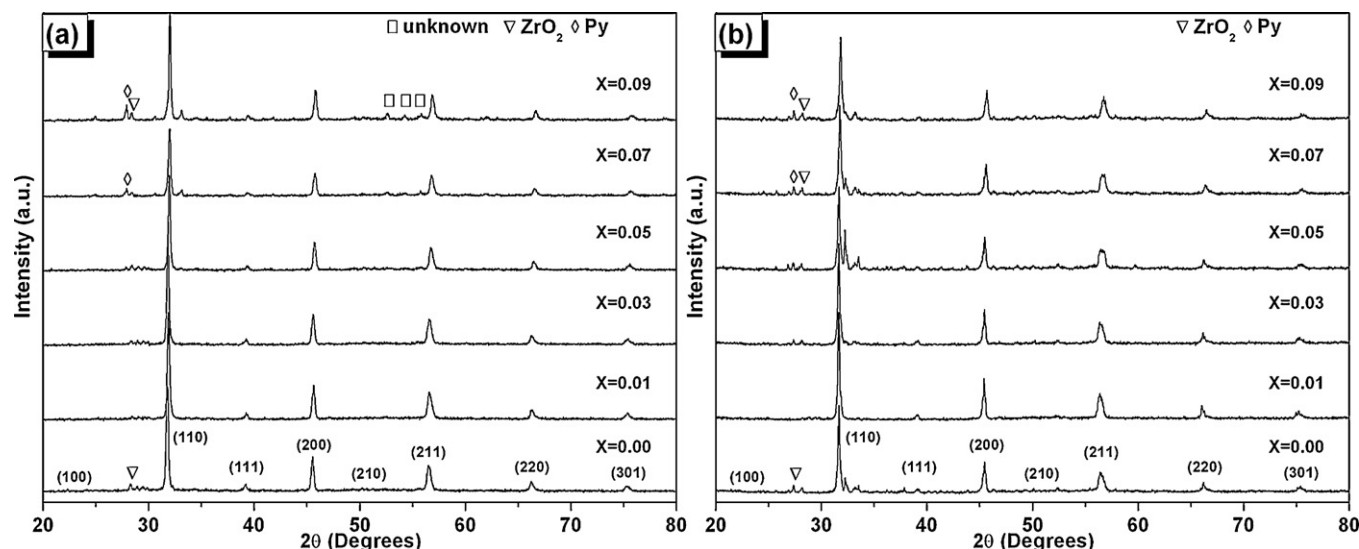


Fig. 1. X-ray diffraction patterns of $[\text{Bi}_{0.5}\text{Na}_{0.5}]_{1-x/2}[\text{Ti}_{0.41}\text{Zr}_{0.59}]_{1-x}\text{Nb}_x\text{O}_3$ (a) calcined powders and (b) sintered ceramics.

ball-milling media for 24 h. After drying, the calcination was carried out at 700 °C/2 h. Phase development and crystallographic structure of the powders were examined using an X-ray diffractometer (XRD, Philip Model X-pert) with $\text{CuK}\alpha$ radiation. The calcined powders were uniaxially pressed at a pressure of 5.5 MPa with a few drops of 3 wt% polyvinyl alcohol (PVA) used as a binder and then pressed into pellets before being sintered at 900 °C for 2 h and re-checked for phase purity by X-ray diffraction analysis. The density and microstructure of ceramics were evaluated by Archimedes' method and scanning electron microscopy (SEM, JEOL JSM-6335F), respectively. The grain size was determined from the SEM micrographs using the mean linear interception technique. Electrical resistivity measurement was determined using a four-point probe high-resistance meter (Keithley, model 6517A). Dielectric constant (ϵ_r) and loss tangent ($\tan \delta$) were measured at room temperature with frequency in between 1 and 1000 kHz using a LCZ meter (LF Impedance Analyzer 4292A).

3. Results and discussion

X-ray diffraction patterns of $[\text{Bi}_{0.5}\text{Na}_{0.5}]_{1-x/2}[\text{Ti}_{0.41}\text{Zr}_{0.59}]_{1-x}\text{Nb}_x\text{O}_3$ (when $x = 0.00, 0.01, 0.03, 0.05, 0.07$ and 0.09 mol fraction) powders and ceramics are shown in Fig. 1(a) and (b), respectively. Starting from $x = 0.00$, X-ray peaks were indexed to be those of rhombohedral (or pseudo-cubic) structure. In ceramic sample, small amount of impurity peaks were also present. These seemed to belong to ZrO_2 which might precipitate out during sintering at high temperature. In calcinated Nb-doped BNTZ powder, the rhombohedral structure was maintained but there was a slight shift of peaks to the right. This indicated that the unit cell size was slightly reduced. Since the ionic radius of Nb^{5+} ($r = 0.64 \text{ \AA}$ [14]) is larger than that of Ti^{4+} ($r = 0.605 \text{ \AA}$ [14]) but smaller than Zr^{4+} ($r = 0.72 \text{ \AA}$ [14]), it was more likely that Nb^{5+} preferably substituted Zr^{4+} , causing a slight contraction of the unit cell as well as the presence of ZrO_2 in the calcined powder when Nb concentration was above 0.05 mol fraction. In Nb-

doped BNTZ ceramics, starting from $x = 0.05$, small amount of pyrochlore phase and ZrO_2 began to show in X-ray diffraction patterns. Such small solubility limit and similar impurity phases were also observed in Nb-doped PZT system [5]. Nevertheless, the slight shift of X-ray peaks to the right was still observed in the ceramic samples, indicating that Nb substitution in Zr sites still occurred.

The densities of undoped and Nb-doped ceramics as a function of Nb content are shown in Fig. 2. Addition of 0.01 mol fraction of Nb caused a decrease in density value. It was observed by inspection that this sample had rather weak grain boundaries causing grains to be easily loosened compared to other samples. To study the cause of this grain boundary weakening would need careful investigation of the grain boundaries by transmission electron microscopy. Nevertheless, the rest of the samples in this study showed relative densities ranging from 92% to 96% of their theoretical values. The effect of Nb addition on microstructure is shown in Fig. 3. In general, increasing Nb concentration caused average grain size to

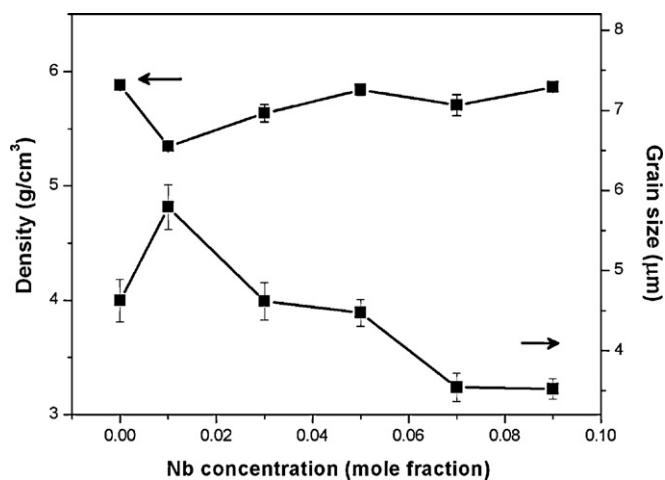


Fig. 2. The density and grain size of $[\text{Bi}_{0.5}\text{Na}_{0.5}]_{1-x/2}[\text{Ti}_{0.41}\text{Zr}_{0.59}]_{1-x}\text{Nb}_x\text{O}_3$ ceramics.

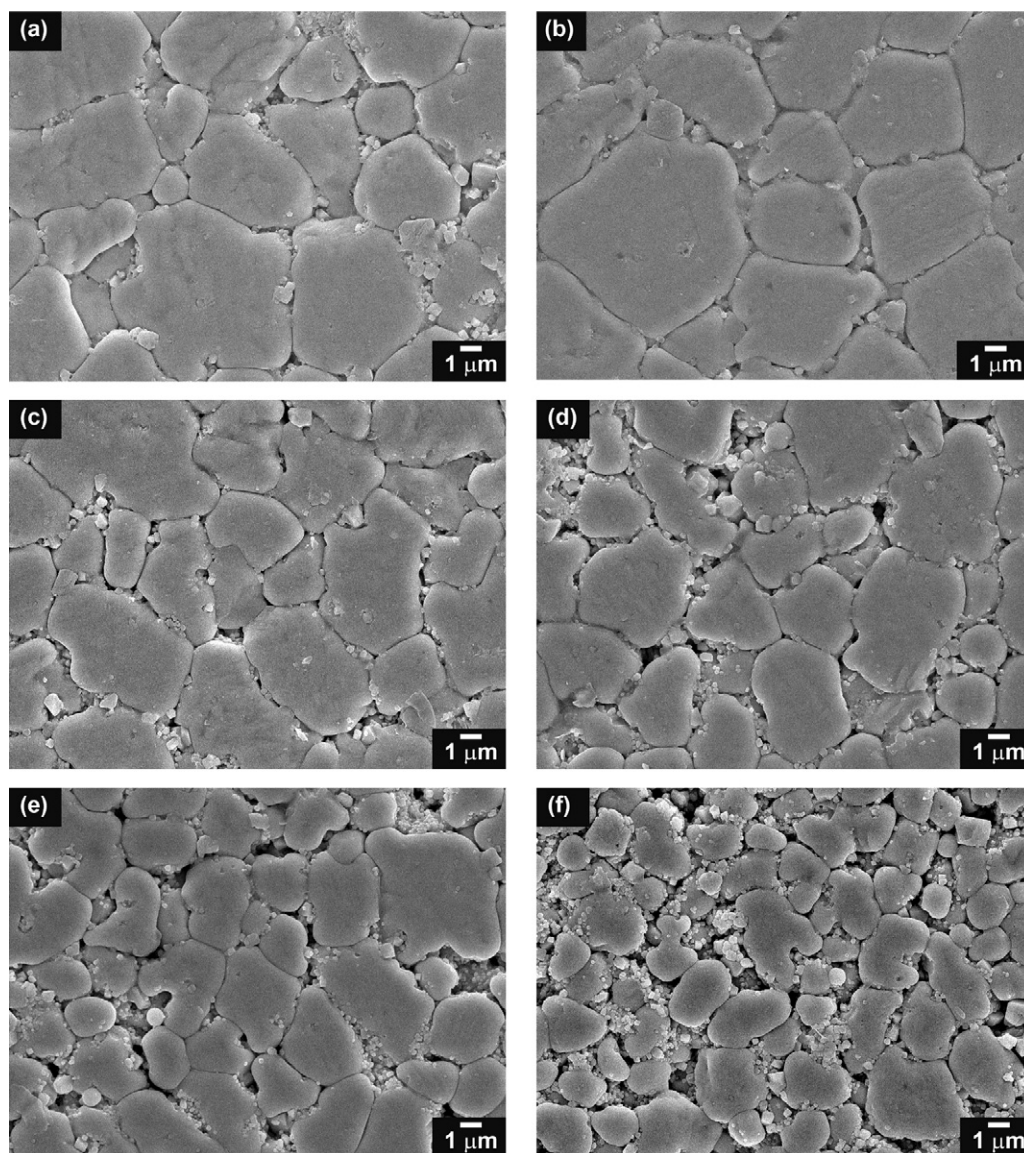


Fig. 3. The microstructure of $[\text{Bi}_{0.5}\text{Na}_{0.5}]_{1-x/2}[\text{Ti}_{0.41}\text{Zr}_{0.59}]_{1-x}\text{Nb}_x\text{CrO}_3$ ceramics when (a) 0.00, (b) 0.01, (c) 0.03, (d) 0.05, (e) 0.07 and (f) 0.09 mol fraction.

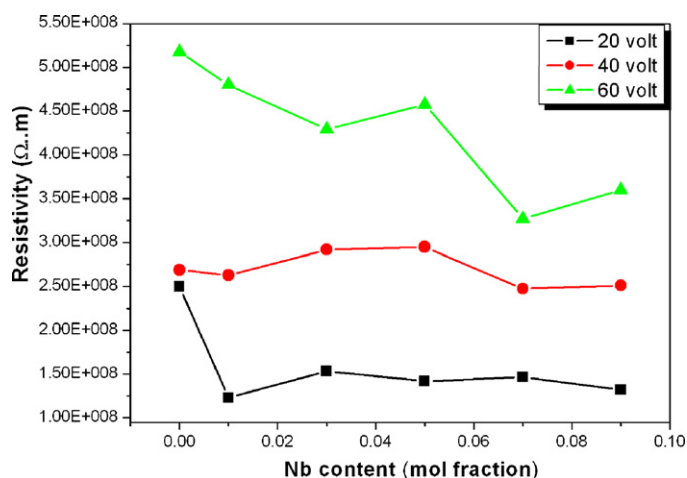


Fig. 4. The variation of room temperature dc resistivity as a function of Nb concentration and applied voltage.

decrease from 5.79 μm in BNTZ ceramic to 3.52 μm in BNTZ/0.09Nb ceramic (Fig. 2). This grain growth inhibition seemed to be typical and was also observed in other donor-doped systems, for example, Nb-doped BaTiO_3 [15] and Nb-doped PZT [5]. The space charge produced from higher valent Nb^{5+} ion was expected to play a key role in grain growth mechanism of this type of compound.

Fig. 4 shows the variation of room temperature dc resistivity as a function of Nb concentration and applied voltage. It can be seen that, for a given applied voltage, the electrical resistivity had roughly a decreasing trend when Nb concentration increased, indicating that Nb provided more electrons to BNTZ ceramic. However, Hall effect measurement should be carried out to correctly determine the major charge carriers in these compounds. Nevertheless, the absolute values of resistivity for undoped and Nb-doped BNTZ ceramics were of the same order i.e. $\sim 10^8 \Omega\text{m}$ which suggested that Nb concentration affected only slightly the intrinsic electrical

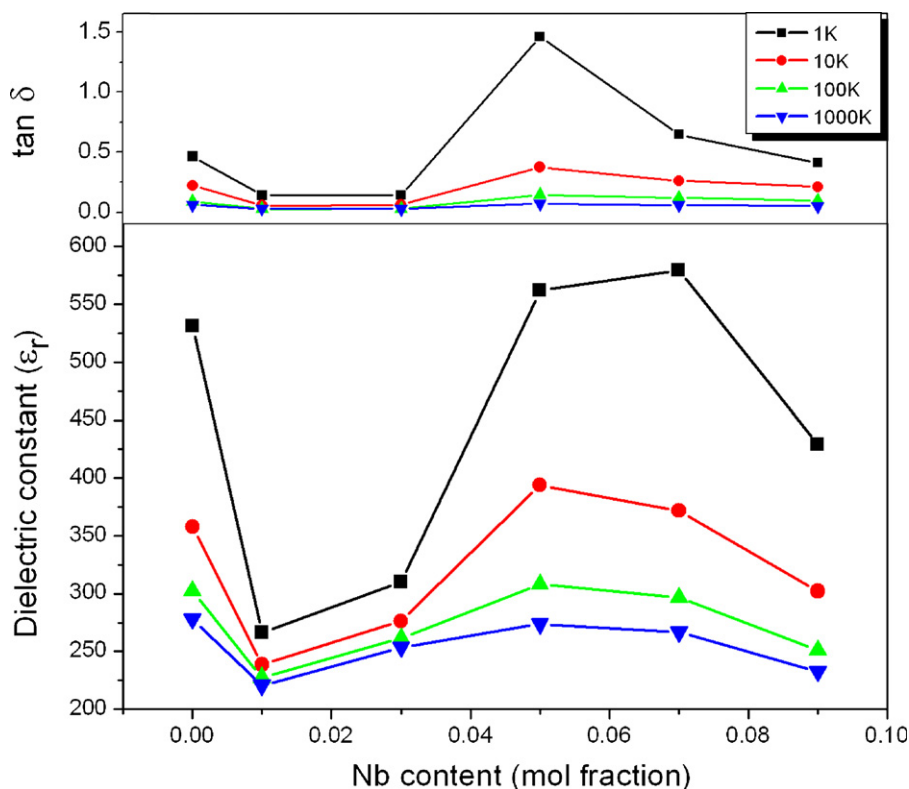


Fig. 5. The variation of room temperature dielectric constant (ϵ_r) and dielectric loss ($\tan \delta$) with Nb concentrations and frequencies.

resistivity of these compounds. Similar magnitude of resistivity was also observed in BNT-BT system [16]. An increase in applied voltage caused a slight increase in resistivity although the values were still in the same order as those at lower voltages. This was an indication of non-linear behavior of electrical conduction in this a dielectric material.

Fig. 5 showed the variation of room temperature dielectric constant (ϵ_r) and dielectric loss ($\tan \delta$) with Nb concentrations and frequency. Addition of small concentration of 0.01 and 0.03 mol fraction of Nb caused a drop in dielectric constant. This may partially be correlated to the relatively lower densities of these samples coupled with a decrease in electrical resistivity. A further increase in Nb resulted in an increase in dielectric constant and then dropped off again. There seemed to be several competing factors determining the room temperature dielectric behavior of Nb-doped BNTZ ceramics. The most important ones included the ease of domain wall movement due to donor-type doping and the decrease in grain size. The presence of higher fraction of grain boundaries in the ceramic would reduce the efficiency of dipole alignment. In our samples, the optimized composition for dielectric properties was found at 0.05–0.07 Nb mol fraction.

4. Conclusions

Lead-free $[\text{Bi}_{0.5}\text{Na}_{0.5}]_{1-x/2}[\text{Ti}_{0.41}\text{Zr}_{0.59}]_{1-x}\text{Nb}_x\text{O}_3$ (where $x = 0.00, 0.01, 0.03, 0.05, 0.07$ and 0.09) were successfully fabricated. X-ray diffraction patterns showed rhombohedral (or pseudo-cubic) structure. Addition of Nb caused a slight lattice contraction indicating its preference in substituting for Zr sites.

All ceramic samples showed dense microstructure while grain size tended decrease with increasing Nb concentration. The magnitude of the electrical resistivity of both undoped and doped samples was nearly the same i.e. $\sim 10^8 \Omega \text{ m}$ with observed non-linear behavior. The relationship between dielectric properties and composition was found to have no particular trend but they seemed to be optimized at 0.05–0.07 Nb mol fraction.

Acknowledgements

This work is financially supported by the Thailand Research Fund (TRF), the National Research University Project under Thailand's Office of the Higher Education Commission (OHEC). The Faculty of Science and the Graduate School, Chiang Mai University is also acknowledged. Ms. Ampika Rachakom would like to thank the Commission on Higher Education for supporting by grant fund under the program Strategic Scholarships for Frontier Research Network for the Ph.D. Program Thai Doctoral degree for this research. The authors would also like to thank Asst. Prof. Dr. Rattikorn Yimnirun, School of Physics, Institute of Science, Suranaree University of Technology for provision of electrical measurements.

References

- [1] B. Jaffe, W.R. Cook, H. Jaffe, *Piezoelectric Ceramics*, Academic press, London, United Kingdom, 1971.
- [2] G.H. Haertling, *Ferroelectric ceramics: history and technology*, *Journal of the American Ceramic Society* 82 (1999) 797–818.

- [3] A.J. Moulson, J.M. Herbert, *Electroceramics*, second ed., John Wiley & Sons, Chichester, 2003.
- [4] J. Rudolph, Mechanism of conduction in oxide semiconductors at high temperatures, *Zeitschrift für Naturforschung* 14 (1959) 727–737.
- [5] C.-L. Huang, B.-H. Chen, L. Wu, Variability of impurity doping the modified $\text{Pb}(\text{Zr}, \text{Ti})\text{O}_3$ ceramics of type ABO_3 , *Solid State Communications* 130 (2004) 19–23.
- [6] M. Pereira, A.G. Peixoto, M.J.M. Gomes, Effect of Nb doping on the microstructure and electrical properties of the PZT ceramics, *Journal of the European Ceramic Society* 21 (2001) 1353–1356.
- [7] S.-Y. Chu, T.Y. Chen, I.-T. Tsai, W. Water, Doping effects of Nb additives on the piezoelectric and dielectric properties of PZT ceramics and its application on SAW device, *Sensors and Actuators* 113 (2004) 198–203.
- [8] Md.A. Mohiddon, R. Kumar, P. Geol, K.L. Yadav, Effect of Nb doping on structural and electric properties of PZT (65/35) ceramics, *IEEE Transactions on Dielectrics and Electrical Insulation Society* 14 (2007) 204–211.
- [9] T. Maiti, R. Guo, A.S. Bhalla, The evolution of relaxor behavior in Ti^{4+} doped BaZrO_3 ceramics, *Journal of Applied Physics* 100 (2006) 1141091–1141096.
- [10] X.G. Tang, K.-H. Chew, H.L.W. Chan, Diffuse phase transition and dielectric tunability of $\text{Ba}(\text{Zr}_y\text{Ti}_{1-y})\text{O}_3$, *Acta Materialia* 52 (2004) 5177–5183.
- [11] T. Takenaka, H. Nagata, Y. Hiruma, Y. Yoshii, K. Matumoto, Lead-free piezoelectric ceramics based on perovskite structures, *Journal of Electroceramics* 19 (2007) 259–265.
- [12] Z. Chen, J. Hu, Piezoelectric and dielectric properties of $(\text{Bi}_{0.5}\text{Na}_{0.5})_{0.94}\text{Ba}_{0.06}\text{TiO}_3\text{--Ba}(\text{Zr}_{0.04}\text{Ti}_{0.96})\text{O}_3$ lead-free piezoelectric ceramics, *Ceramics International* 35 (2009) 111–115.
- [13] Y. Yamada, T. Akutsu, H. Asada, K. Nozawa, S. Hachiga, T. Kurosaki, O. Ikagawa, H. Fujiki, K. Hozumi, T. Kawamura, T. Amakawa, K.-I. Hirota, T. Ikeda, Effect of B-ion substitution in $[(\text{K}_{1/2}\text{Bi}_{1/2})\text{--}(\text{Na}_{1/2}\text{Bi}_{1/2})](\text{Ti--B})\text{O}_3$ system with $\text{B} = \text{Zr}, \text{Fe}_{1/2}, \text{Nb}_{1/2}, \text{Zn}_{1/3}\text{Nb}_{2/3}$ or $\text{Mg}_{1/3}\text{Nb}_{2/3}$, *Japanese Journal of Applied Physics* 34 (1995) 5462–5466.
- [14] R.D. Shannon, Revised effective ionic radii and systematic studies of interatomic distances in halides and chalcogenides, *Acta Crystallographica* 32 (1976) 751–767.
- [15] E. Brzozowski, M.S. Castro, Grain growth control in Nb-doped BaTiO_3 , *Journal of Materials Processing Technology* 168 (2005) 464–470.
- [16] B.-J. Chu, J.-H. Cho, Y.-H. Lee, B.-I. Kim, D.-R. Chen, The potential application of BNT based ceramics in large displacement actuation, *Journal of Ceramics Processing Research* 3 (2002) 231–243.